AQUA
Water Infrastructure, Ecosystems and Society

 AQUA — Water Infrastructure, Ecosystems and Society Vol 71 No 4, 563 doi: 10.2166/aqua.2022.005

Experimental study on pressure characteristics of direct water hammer in the viscoelastic pipeline

Xiaoying Zhang[a], Sheng Chen[b], Tingyu Xu[b,*] and Jian Zhang[b]

[a] College of Hydraulic and Civil Engineering, Xinjiang Key Laboratory of Hydraulic Engineering Security and Water Disasters Prevention, Xinjiang Agricultural University, Urumqi 830052, China
[b] College of Water Conservancy and Hydropower Engineering, Hohai University, Nanjing 210098, China
*Corresponding author. E-mail: Tingyu_hhu@163.com

ABSTRACT

With the increasing popularity of long-distance water supply projects and the development of materials technology, the variation of water hammer characteristics in the viscoelastic pipeline has become the focus of researchers. To find out the mechanism of water hammer in the viscoelastic pipe of both elastic and viscous properties, an experiment was set up to study the direct water hammer generated by rapid closure of the downstream valve in the polymethyl methacrylate (PMMA) pipe, with six flow velocities in nearly 70 tests. The experimental results showed that the maximum water hammer pressure generated in the viscoelastic pipe in all flow velocities was (20% at most) greater than the traditional value of Joukowsky's formula. A faster closing time of the valve caused a higher water hammer pressure. The difference in water hammer pressure generated between the fastest and the slowest closing time of the valve was 14–17% at each flow velocity. Based on the relationship between the stress and strain of the pipe wall in the viscoelastic pipe, the reason that the water hammer characteristic in the viscoelastic pipeline was different from the traditional value was explained. The study provides a reference for the mechanism of transient flow in viscoelastic pipelines.

Key words: closing time of the valve, direct water hammer pressure, transition process, viscoelastic pipe

HIGHLIGHTS

- An experiment of direct water hammer generated by rapid closure of valve was conducted in a long and straight PMMA pipe.
- Measured maximum water hammer pressure rise was 15–20% greater than the traditional value of Joukowsky's formula.
- A faster closing time of the valve caused a higher direct water hammer pressure.

GRAPHICAL ABSTRACT

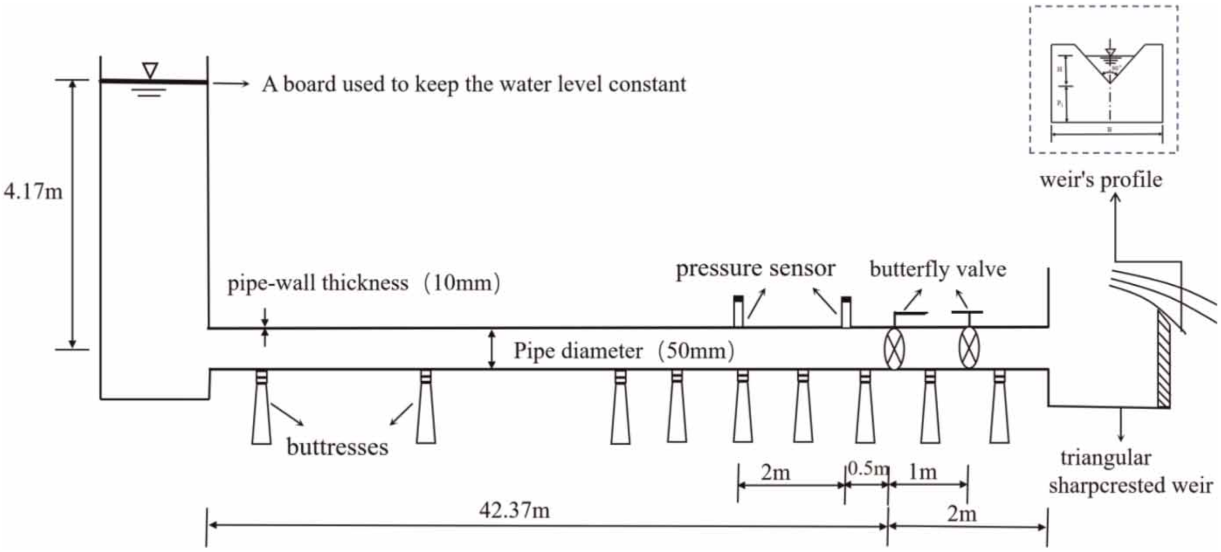

INTRODUCTION

In the long-distance water conveyance project with large flow rate, long line, large pipe diameter and large pressure, the pipeline system involving all kinds of valves, chambers and pump stations may cause huge water hammer pressure due to any improper operation reasons, which may cause serious harm to the whole system (Chaudhry 1979; Wylie *et al.* 1993). Then, many researchers studied how to arrange protective measures for excessive water hammer pressure in steel pipes to ensure safety (Thorley 2004; Miao *et al.* 2017; Tran 2017; Chen *et al.* 2021).

With the rapid development of materials technology, some new types of viscoelastic pipes with a series of advantages in low cost, lightweight and corrosion resistance have been increasingly used throughout the world for potable water distribution, sewage effluent transport and agriculture irrigation (Covas *et al.* 2004; Bergant *et al.* 2008; Duan *et al.* 2010). Meanwhile, the popularity of some new types of viscoelastic material pipes, such as support pipe (SP), ductile iron pipe (DIP), polyvinyl chloride (PVC) pipe, prestressed concrete cylinder (PCCP) pipe, polyethylene (PE) pipe, polypropylene (PP) pipe, fiber-reinforced plastic mortar (FRPM) pipe, high-density polyethylene (HDPE) pipe and so on, is also increasing in long-distance water conveyance projects in Xinjiang, China. For example, the FRPM pipe was used for the Small Sink Inverted Siphon Project; the combined scheme of the PCCP and the SP was adopted for the Sangequan Inverted Siphon Project; the combined scheme of the SP and FRPM pipe was adopted in the Luobupo Potassium Salt External Water Conveyance Project; the combined scheme of the DIP and SP was adopted in the main line of the Daxigou Pipeline Water Diversion Project in 2015.

Any deformation of polymer molecules in polymethyl methacrylate (PMMA) pipe in accordance with the stress cannot be completed instantaneously under the action of external forces, and the mechanical properties have significant viscoelastic characteristics. This kind of pipe is called viscoelastic pipe. Compared with traditional elastic pipes, viscoelastic pipes have both elastic and viscous characteristics. Under the action of stress, the viscoelastic pipe produces not only similar instantaneous strain to the elastic material, but also partial lags behind that of stress–strain (Franke 1983; Wineman & Rajagopal 2000; Covas *et al.* 2004; Gong *et al.* 2016; Pan *et al.* 2020). Recently, the influence of the viscoelastic deformation of pipe wall on the transient flow response of pipelines was studied through numerical simulation and physical tests, and the viscoelastic models were applied to leakage, partial, blockage, ill-junction and so on (Duan *et al.* 2020; Pan *et al.* 2020). Most models were based on the delay time scale (τ) and creep compliance (J) of the Kelvin–Voigt model (Gally *et al.* 1979; Duan *et al.* 2010; Pezzinga *et al.* 2016). The numerical and experimental studies have been conducted for viscoelastic responses in plastic or polymeric pipelines (Gong *et al.* 2018; Triki 2018; Urbanowicz *et al.* 2019). These experimental results showed that the deformation rate of viscoelastic pipe was much higher than that of elastic pipe, and the viscoelastic pipe may be able to bear more severe pressure rise than elastic pipe. At the same time, the viscoelastic effect induces a time-delay or phaseshift in transient responses. It is very important to determine the viscoelastic parameters in the viscoelastic pipe for transient flow modeling and analysis when using the viscoelastic pipe.

The transient theory and models have been applied with substantial progress and achievement for traditional elastic pipes, such as one-dimensional (1D) and two-dimensional (2D) water hammer models, unsteady friction or turbulence models (Trikha 1975; Vardy & Brown 1995; Brunone & Golia 2008; Duan *et al.* 2018). As for the hydraulic transition process of long-distance water supply engineering, researchers mostly used the above-mentioned traditional elastic pipes' transient theory and models to study the hydraulic transition process of elastic pipelines, such as concrete and steel. Many schemes to reduce water hammer pressure have been put forward and applied to practical projects. However, the viscoelastic effect of PVC, PCCP, PE and other pipes was seldom considered at present in the design scheme of safe operation of water supply projects. Only the lateral and axial strains of the tube wall were considered in the calculation of wave velocity. The transient flow theory of the elastic pipeline was still used as the basis for water supply engineering design, and the calculation formula of direct water hammer pressure was still the traditional formula. If the study of the hydraulic transition process in the viscoelastic pipeline is not sufficient, and the actual engineering fails to meet the requirements of design and operation, serious water hammer accidents will occur, causing great hidden dangers of personal safety and economic losses. Therefore, the understanding of transient flow in the viscoelastic pipeline should be improved. The effect of the wall elasticity and viscosity on the water hammer pressure remains to be further studied.

Based on physical tests of water hammer characteristics in PMMA pipe, this study aims to examine the variation of direct water hammer, as well as the influence of the closing time of the downstream valve in the viscoelastic pipe, and extend the results to provide a theoretical basis for water hammer prevention and safe operation of viscoelastic pipe. The paper starts with the experimental method. The physical tests were conducted with both the same closing time under different flow velocities and the different closing times of the valve under the same flow velocity. Then, the experimental data were compared with the traditional water hammer theory, and the reason for the difference in the direct water hammer characteristic in the viscoelastic pipeline was also discussed. Also, the influence of the closing time on direct water hammer pressure in the viscoelastic pipeline was explained. Finally, the key findings and future work are summarized in the conclusion.

METHOD

The test apparatus consisted of an upstream water tank, a PMMA pipe, a midline butterfly valve, a flow regulating valve and a downstream water tank. The physical test schematic diagram is shown in Figure 1. The PMMA pipe was 44.37 m in length with 5 cm inner diameter of the pipe. To measure the water hammer pressure, the high-frequency dynamic pressure sensors were installed at the positions of 0.5 and 2 m in front of the butterfly valve in the middle line of the end, respectively. The distance between the butterfly valve and the upstream water tank was 42.37 m. The distance between the butterfly valve and the downstream water tank was 2 m. The overflow plate was arranged in the upstream water tank to ensure the upstream water level was constant. A 90° open triangular thin-walled weir was arranged in the downstream tank to measure the flow in the pipeline. The regulating valve was arranged behind the butterfly valve to adjust the flow of the pipeline. A support pier was installed every 1 m along the pipeline to prevent vibration and displacement of the pipeline during valve closure.

The physical test was mainly carried on the water hammer of rapid closure of valve under the different flow velocities. To ensure that the flow pattern in the pipe was turbulent, the minimum flow velocity of the pipe was 0.11 m/s. When the flow velocity of the pipe exceeded 0.29 m/s, clusters of bubbles were clearly observed to precipitate in the test pipe, resulting in liquid column separation. Therefore, the flow velocity of this test was between 0.11 and 0.29 m/s. Three methods were used to determine the flow velocity simultaneously, including 90° triangle thin-walled weir, ultrasonic flowmeter and weighing method. The flow velocity error of the three methods was proved to be within $\pm 5\%$ by experiments. The water temperature was measured before each test, ranging from 13 to 15 °C. A high-frequency and high-precision dynamic pressure sensor (GYG1405F) was used to measure the pressure of the pipeline. The accuracy level of the pressure sensor was 0.5% F.S and the frequency response was 20 kHz. The CRAS data monitoring and collection system independently developed by Nanjing Founder Company was adopted to collect the water hammer pressure data with a collection frequency of 25.6 kHz, that was, 25,600 times of data could be collected within 1 s. The collection duration of the first group of experiments in this experiment was set as 6 s. For the direct water hammer test, the valve was required to be closed immediately. According to Formula (1), the direct water hammer could only be generated in the pipe when the closing time of the valve was less than 0.12 s. The closing time of the electric valve was too close to the closing time of the valve limited by the direct water hammer, so the test

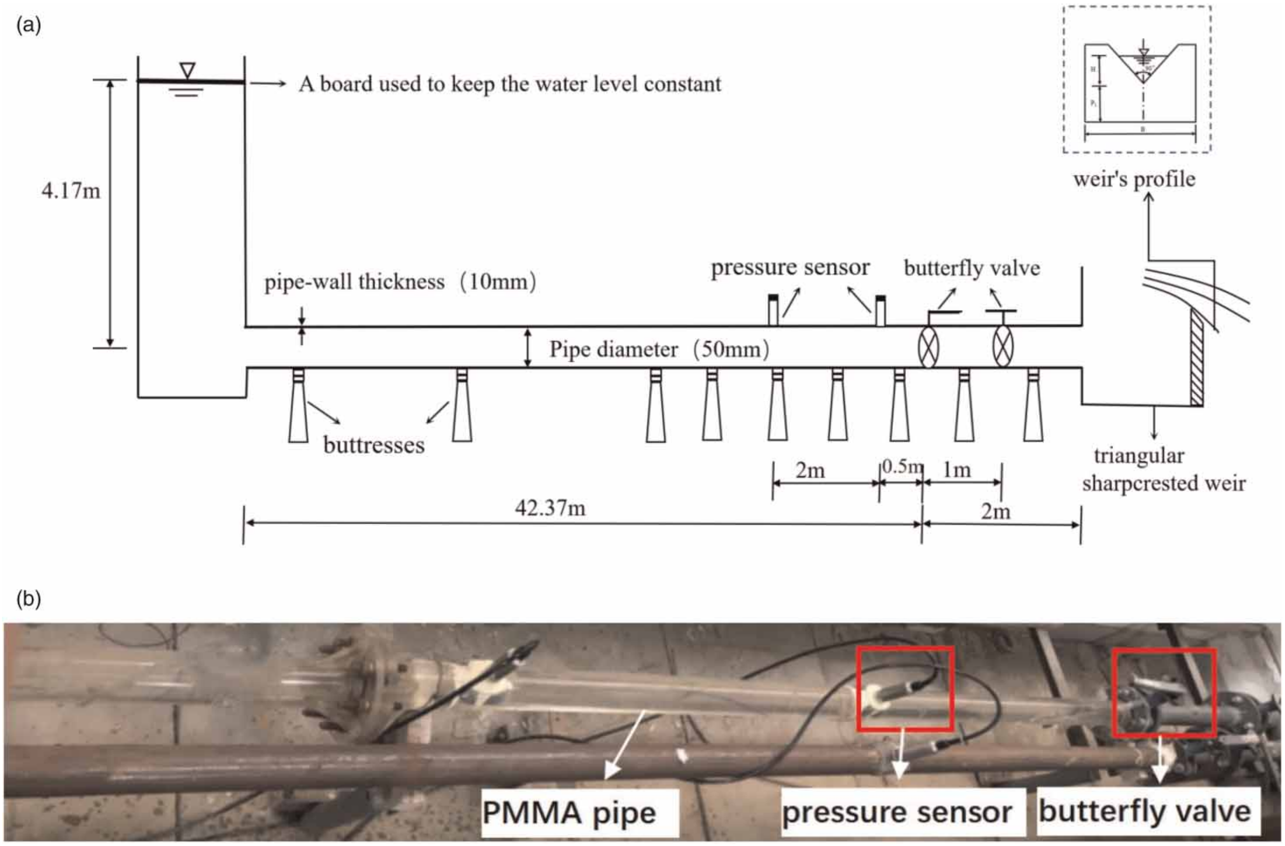

Figure 1 | Layout of test equipment: (a) test layout diagram and (b) testing the PMMA pipe system.

can only be carried out by closing the valve manually. A specialized experimenter was trained to close the downstream valve as quickly as possible, around 40 ms, to guarantee a direct water hammer generated in the pipe. At least 10 rapid valve closing tests were conducted for each flow velocity. The first five times of tests were conducted at the most quick velocity and the last five times of tests were conducted at a slightly slow velocity for different valve closing times. The closing time of the valve was compared. The experimental data were the same under the same closing time of the valve. The water hammer pressure waveform and extreme value should be basically consistent, indicating that the experimental data could be repeatedly verified. Tests were carried out in six different flow velocities (0.11, 0.147, 0.183, 0.216, 0.247 and 0.284 m/s).

RESULTS AND DISCUSSION

Comparison between experimental data and traditional results

According to Formula (1) of the traditional water hammer theory, the direct pressure values of water hammer theory at different flow velocities were calculated as shown in Table 1. The calculation of wave velocity was based on Formula (2) of wave velocity, and the calculated wave velocity in this test pipeline was 637 m/s.

$$\Delta H = -\frac{a}{g}\Delta V \tag{1}$$

where ΔH was the water hammer pressure, m; a was the wave velocity, m/s; g was the acceleration of gravity, m/s^2 and ΔV was the velocity variation, m/s.

$$a = \frac{\sqrt{K/\rho}}{\sqrt{1+[(K/E)(D/e)]c_1}} = \frac{1{,}435}{\sqrt{1+[(2.2\times10^9/2.7\times10^9)(0.05/0.01)]}} = 637\ \mathrm{m/s} \tag{2}$$

Table 1 | Pressure rise of direct water hammer at different flow velocities

Velocity (m/s)	0.110	0.147	0.183	0.216	0.247	0.284
ΔH (m)	7.14	9.55	11.88	14.03	16.04	18.44

where the elastic modulus of water was $K = 2.2 \times 10^9$ Pa; water density was $\rho = 1{,}000$ kg/m^3; the elastic modulus of the PMMA pipe was $E = 2.7 \times 10^9$ Pa. The diameter of the pipe in this experiment was 0.05 m; the wall thickness was 0.01 m; all PMMA pipes were connected by expansion joints, so the value of c_1 was 1.

The physical test conditions are shown in Table 2. The relationship between the experimental data at six different flow velocities (0.110, 0.147, 0.183, 0.216, 0.247 and 0.284 m/s) and the traditional values calculated by Formula (1) are shown in Figure 2.

As shown in Figure 2, when the flow velocity was constant, the shapes of water hammer waves by rapidly closing the downstream valve of any three groups were basically identical. The propagation periods of water hammer waves were also the same. The experimental data at each flow velocity showed the repeatability. The maximum pressure rise at each flow velocity was all greater than the traditional value as Equation (1). When $V = 0.11$ m/s (Figure 2(a)), the traditional pressure rise was 7.14 m. In the physical test of water hammer of rapid closure of valve in the PMMA pipe, the measured pressure rises were 8.48, 8.57 and 8.57 m, respectively. The maximum pressure rise among them was 1.43 m (20.03%) higher than the traditional value. When $V = 0.147$ m/s (Figure 2(b)), the traditional pressure rise was 9.55 m. In the physical test of water hammer of rapid closure of valve in the PMMA pipe, the measured pressure rises were 11.37, 11.40 and 11.38 m. The maximum pressure rise among them was 1.85 m (19.37%) higher than the traditional value. When $V = 0.183$ m/s (Figure 2(c)), the measured pressure rises were 2.25, 2.09 and 2.24 m (18.94% at most), respectively higher than while the traditional water hammer pressure rise (11.88 m). When $V = 0.216$ m/s (Figure 2(d)), the measured pressure rises were 2.20, 2.21 and 2.34 m (16.68% at most), respectively higher than while the traditional water hammer pressure rise (14.03 m). When $V = 0.247$ m/s (Figure 2(e)), the maximum measured pressure rise was 15.21% greater than the traditional value. When $V = 0.284$ m/s (Figure 2(f)), the maximum measured pressure rise was 16.38% greater than the traditional value. At that time, the minimum negative pressure reached -9 m. After careful observation of the phenomenon in the pipe, no visible gas occurred. However, when the flow rate increased a little more, to 0.29 m/s, bubbles were precipitated from the pipe, which indicated that the liquid column separation occurred. In general, the measured pressure rises at different flow velocities in the PMMA pipe were 15–20% greater than the traditional value, which meant that Formula (1) was safe enough and not applicable to the water hammer calculation of the viscoelastic pipeline. During the process of water hammer wave propagation, the maximum water hammer waveform of the first wave was different from the shape of water hammer wave in elastic pipes, such as steel pipe and copper pipe. In the direct water hammer experiment of steel pipe and copper pipe, the first wave shape was a square rectangular wave, while in this experiment, the waveforms of the PMMA pipe first produced a large protruding point and then produced a drop to an approximate flat end. The shape of the waveform of the first negative pressure wave was similar to that of the first positive pressure wave, which should be reflected by the positive pressure wave.

The above test results could be explained by the inherent characteristics of viscoelastic pipe materials. The water hammer wave generated by the rapid closure of the valve in the water conveyance pipeline would not only cause the change of the

Table 2 | Test conditions

Flow velocities (m/s)	Times	Test number (no.)
0.110	11	1-1, 1-2, …, 1-11
0.147	12	2-1, 2-2, …, 2-12
0.183	10	3-1, 3-2, …, 3-10
0.216	13	4-1, 4-2, …, 4-13
0.247	11	5-1, 5-2, …, 5-11
0.284	12	6-1, 6-2, …, 6-12

Note: In test number (no. *X*-*Y*), where *X* refers to the number of flow rate group and *Y* represents the number of valves closing test.

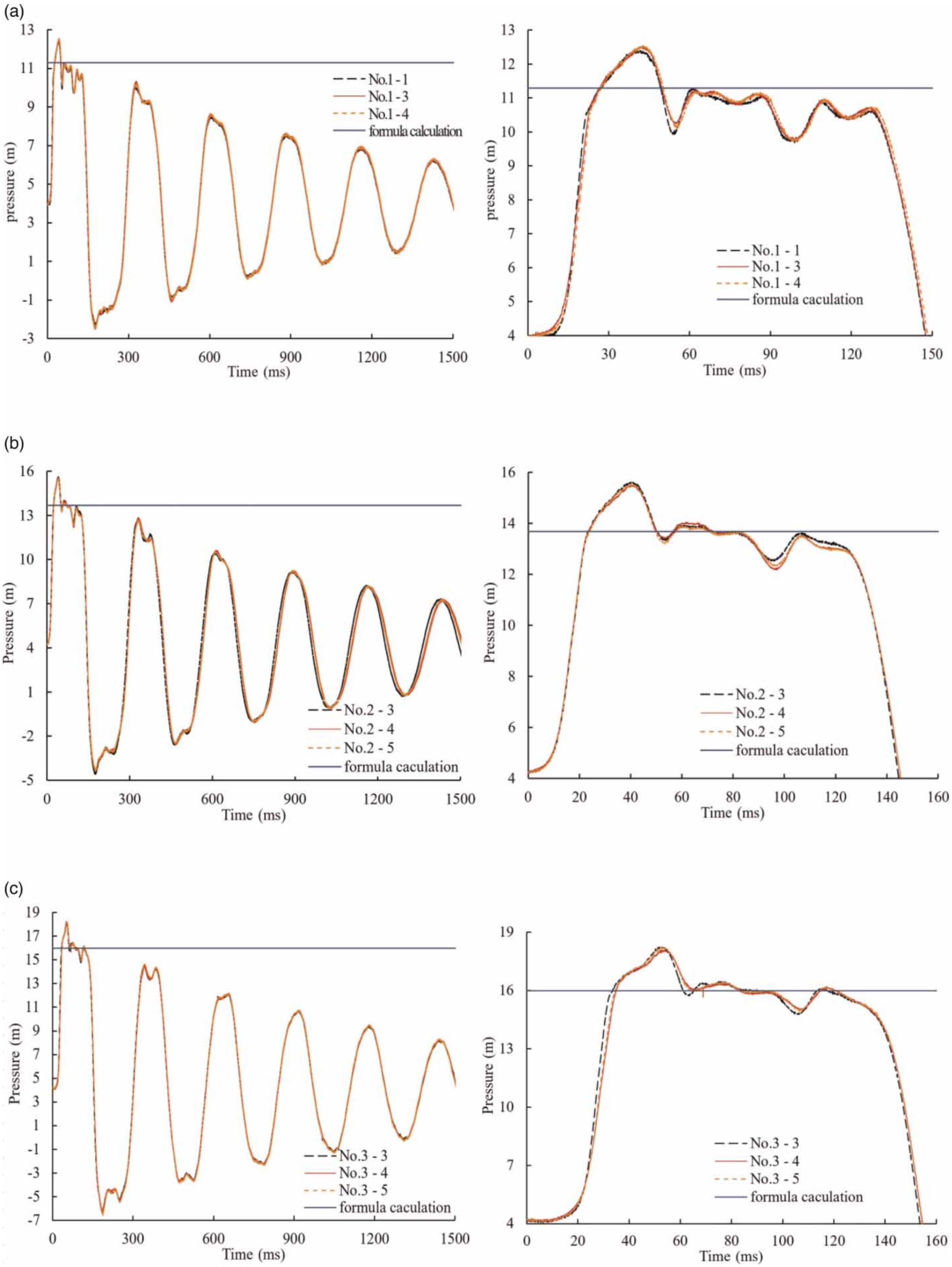

Figure 2 | Comparison of measured and traditional pressure at different flow velocities: (a) $V = 0.11$ m/s; (b) $V = 0.147$ m/s; (c) $V = 0.183$ m/s; (d) $V = 0.216$ m/s; (e) $V = 0.247$ m/s and (f) $V = 0.283$ m/s. (*Continued*).

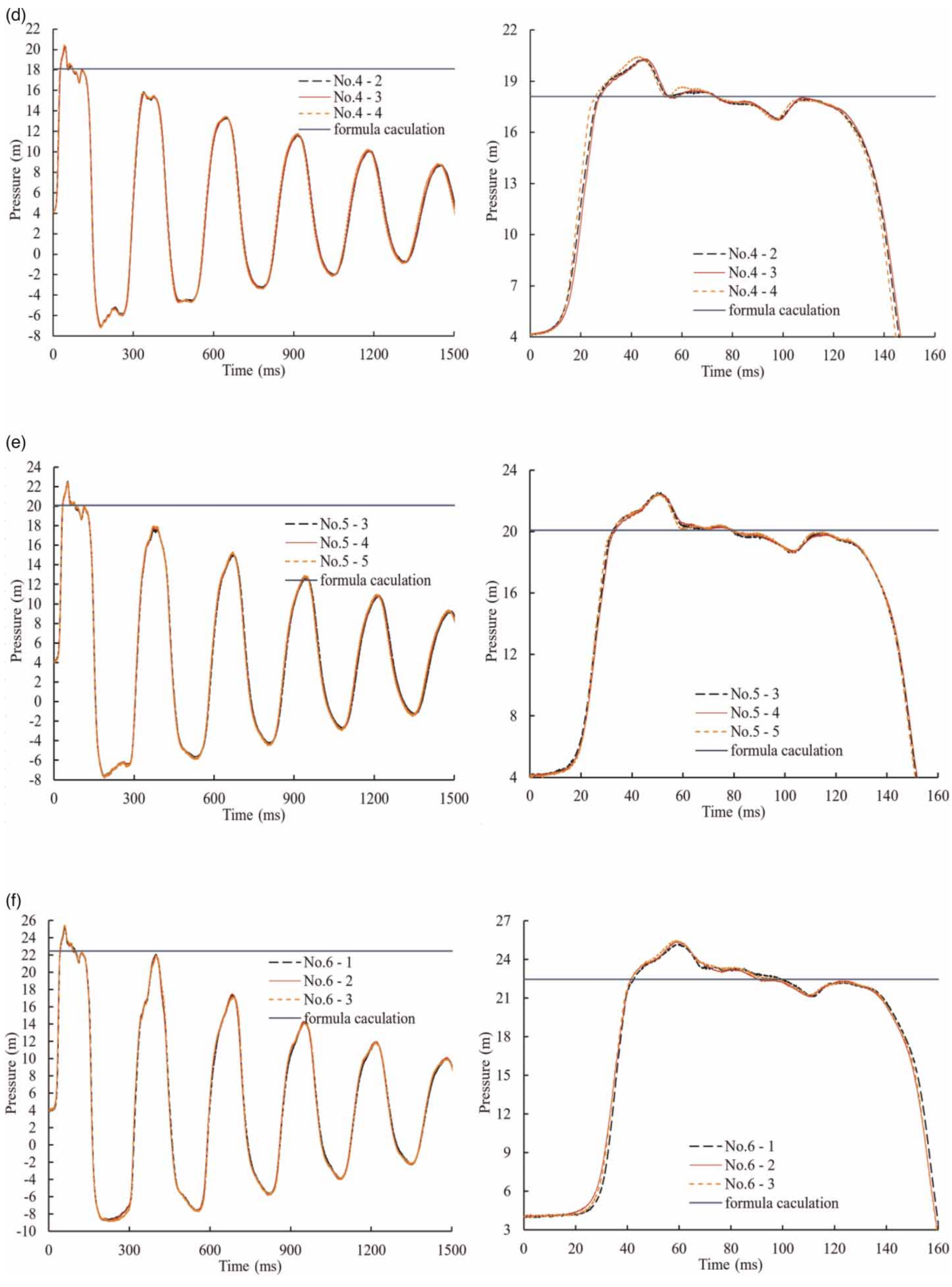

Figure 2 | (*Continued*).

density of water body, but also cause the deformation of the pipeline in its propagation. The medium of water hammer wave propagation was the mixture of the water body and the pipe wall, so the wave velocity in the pipeline under different materials was different. Because of the special properties of the material, the viscoelastic pipe had two kinds of deformation mechanism, namely 'viscous' and 'elastic'. Due to the relatively 'soft' viscoelastic pipe, tube wall deflection was larger. Under the action of stress, viscoelastic material pipe could not only produce similar instantaneous strain and elastic material pipe, but also produce partial lags behind that of stress–strain. Viscoelastic pipe's strain over time is shown in Figure 3. When stress does not change, the relationship between ξ (the viscoelastic pipe strain) and t (time) is shown in Formula (3). ξ increases with t, as shown by curve I in Figure 3. Strain does not occur immediately when the stress is generated, but gradually increases to the maximum value with time. After the stress recedes at t_1, Formula (4) could be obtained from Formula (3), and the strain value gradually decreases with time, as shown by curve II in Figure 3, which indicates that the strain does not disappear instantly, but gradually decreases to 0 with time. When the stress is constant, the strain gradually increases with time. The phenomenon that the strain gradually disappears with time after the stress is removed is called the elastic aftereffect, which is found in pipes of viscoelastic materials, such as PMMA.

$$E = \frac{\sigma}{\xi}\{1 - \exp[-\eta(t - t_0)]\} \tag{3}$$

$$\xi = \xi_1 \exp[-\eta(t - t_1)] \tag{4}$$

where ξ was the strain value, σ was the stress value, E was the elastic modulus of the pipe, $\eta = E/K$ and K was the volumetric elastic modulus of the fluid.

According to the relationship between stress and strain, let $\Delta p/(\Delta A/A) = f(\sigma/\xi)$, it could be known by Formula (3) that when $t = t_0$, $\Delta p/(\Delta A/A) = f(\sigma/\xi) = \infty$, then Formula (5) could be obtained as follows:

$$\frac{1}{f(\sigma/\xi)} = \frac{1}{\infty} = 0 \tag{5}$$

Formula (6) could be obtained from Formula (5):

$$\frac{\Delta A/A}{\Delta p} = 0 \tag{6}$$

Substituting Formula (6) into Formula (2) of wave velocity, Formula (7) could be obtained:

$$a = \sqrt{\frac{K/\rho}{1 + K \times 0}} = \sqrt{K/\rho} = 1{,}483 \text{ m/s} \tag{7}$$

As shown by Curve I in Figure 3, when $t = t_0$, there is no strain in the pipeline, both the rigidity of the pipeline and the elastic modulus are large. As shown by Formula (7), the wave velocity value at this time is 1,483 m/s. When $t = t_1$, the

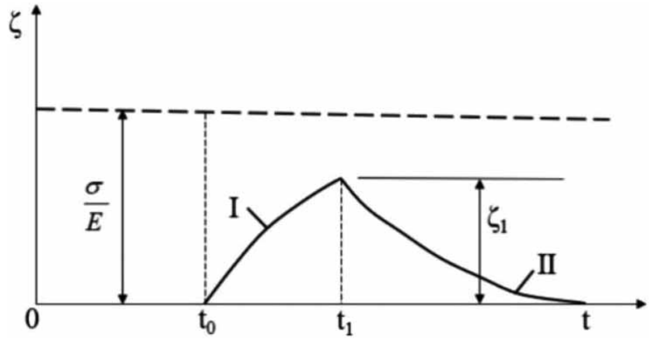

Figure 3 | Strain of a viscoelastic pipe varying with time.

deformation value of the pipeline reaches the maximum, and the corresponding elastic modulus E is the theoretical elastic modulus. In this case, the wave velocity should be the theoretical wave velocity value of 637 m/s. When t varied between t_0 and t_1, the wave velocity value of the pipeline varied between 1,483 and 637 m/s. In the experiment of water hammer of rapid closure of valve, the strain value of the pipeline at the moment of valve closing was small due to the elastic after-effect of the pipeline. According to Formula (3), when the stress is constant, the strain value is inversely proportional to the elastic modulus of the pipeline. The strain decreases, while the rigidity of the pipeline and the elastic modulus of the pipeline increase. According to Formula (2), the wave velocity is not only connected with the characteristics of the water body, the pipe diameter, the pipe wall thickness and the fixed mode, but also related to the elastic modulus of pipe E. When other variables remain unchanged, the greater elastic modulus causes the greater wave velocity. In PMMA pipe, the pressure reaches maximum at the end of time when the valve is closed. At that moment, due to elastic after-effect characteristics of the viscoelastic pipe, the stress without a corresponding strain is produced in the PMMA pipe. After a period of time closing the valve, a high strain occurred in the pipe, which beginning to resist the water effect. The pressure wave attenuates and pressure reduces. Therefore, the measured water hammer pressure waveform first produced bulges, then decreased rapidly and finally approached the flat section.

Influence of closing time of the valve on water hammer in the viscoelastic pipeline

According to the traditional water hammer theory, the direct water hammer has nothing to do with the closing time of the valve. The previous section has verified that the water hammer generated by viscoelastic pipes was greater than the traditional calculated value, indicating that the traditional direct water hammer formula was no longer applicable to the calculation of direct water hammer in viscoelastic pipes, such as PMMA. To find out the influence of closing time of the valve on water hammer, physical tests with different closing times of the valve at the same flow velocity were conducted. Three groups with obvious difference under each flow velocity were chosen to compare with each other. The variation of water hammer at $V = 0.11$ m/s under different closing times of the valve is shown in Figure 4. The measured and traditional pressure rise under different closing times of valve are shown in Table 3. In our experiment, we read the closing time of the valve from the water hammer variation measured by the collected data acquisition system. Before the valve acted, the pressure collected by the pressure sensor should be constant and close to upstream pressure, 4.17 m water head. When the valve started to act, the collected pressure started to rise immediately to the maximum water hammer pressure. Therefore, the effective valve closing time is difference between the time when the pressure reaches the maximum and the time when the pressure begins to rise. The determination of the valve closing time in one test is shown in Figure 5.

Figure 4 shows that the water hammer pressure and the propagation cycle were different under different closing times. When the closing time of the valve decreased, the water hammer transmission cycle decreased, and the water hammer pressure rise increased. As for $V = 0.11$ m/s, the maximum pressure was 12.73 m when the closing time of the valve was

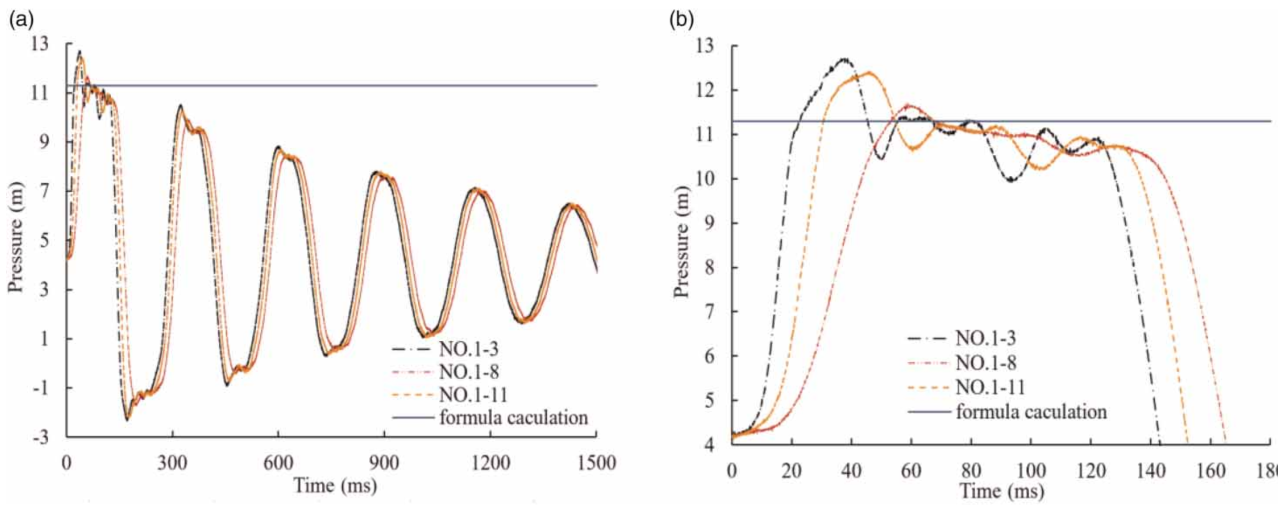

Figure 4 | Comparison of water hammer at flow velocity of 0.11 m/s: (a) multiple cycles and (b) first positive wave.

Table 3 | Measured and traditional pressure rise under different closing times

Average velocity (m/s)	No.	Measured velocity (m/s)	Closure time (ms)	Traditional maximum pressure rise (m)	Measured maximum pressure rise (m)	Difference (m)	(%)
0.110	1–3	0.111	38	7.14	8.58	1.44	20.06
	1–6	0.110	41	7.14	8.48	1.33	18.67
	1–7	0.110	53	7.14	8.07	0.92	12.92
	1–8	0.110	60	7.14	7.55	0.41	5.71
	1–9	0.110	46	7.14	8.28	1.14	15.95
	1–10	0.110	55	7.14	7.75	0.61	8.56
	1–11	0.110	47	7.14	8.27	1.13	15.80
0.183	3–4	0.183	46	11.88	13.97	2.09	17.61
	3–5	0.184	42	11.88	14.12	2.24	18.84
	3–6	0.184	43	11.88	14.06	2.18	18.35
	3–8	0.185	65	11.88	13.15	1.27	10.68
	3–9	0.184	54	11.88	13.36	1.48	12.45
	3–10	0.184	80	11.88	12.11	0.23	1.94
	3–11	0.183	51	11.88	13.59	1.70	14.33
0.284	6–2	0.284	45	18.44	21.36	2.92	15.82
	6–3	0.281	43	18.44	21.46	3.02	16.37
	6–5	0.284	44	18.44	21.36	2.92	15.85
	6–6	0.287	67	18.44	20.46	2.01	10.92
	6–7	0.284	42	18.44	21.61	3.17	17.20
	6–9	0.283	56	18.44	21.24	2.80	15.18
	6–10	0.285	78	18.44	18.90	0.46	2.49

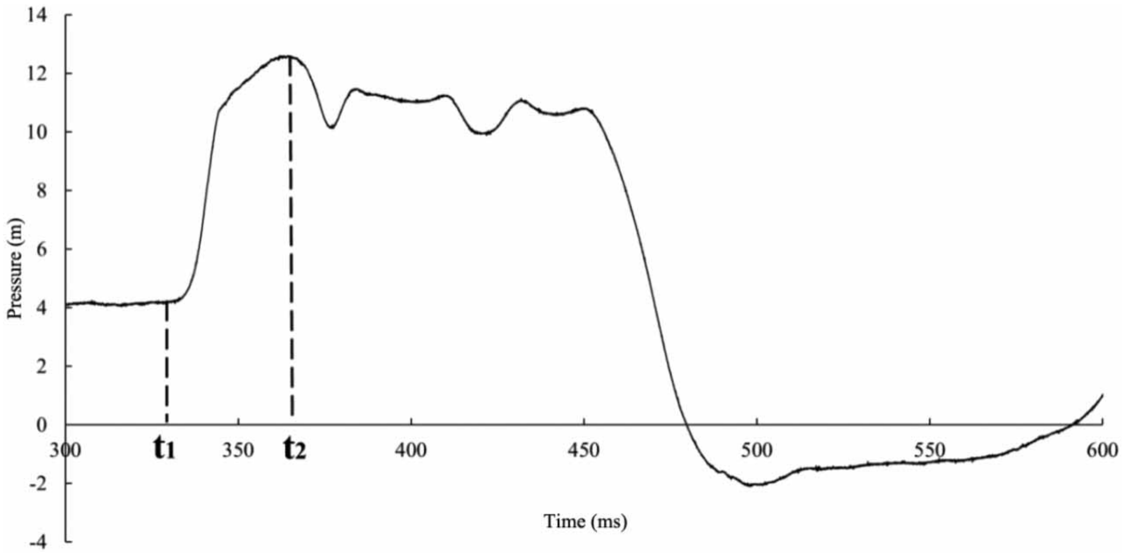

Figure 5 | Determination of the valve closing time in one test. *Note:* $t_2 - t_1$ is the effective closing time of the valve.

38 ms (No. 1-3). The maximum pressure was 11.70 m when the closing time of the valve was 60 ms (No. 1-8). The maximum pressure was 12.42 m when the closing time of the valve was 46 ms (No. 1-11). When the closing time of the valve increased from 38 to 46 ms and then to 60 ms, the water hammer wave propagation period increased from 0.266 to 0.269 s and then to 0.272 s. The maximum pressure decreased from 12.73 to 12.42 m and then to 11.70 m. The pressure rises of three tests of water hammer were 20.06, 15.95 and 5.71% higher than the traditional value, respectively.

Since the maximum pressure of direct water hammer occurred at the end of valve closing, only the relationship between valve closing time and pressure change in the first positive wave length at different flow velocities is shown in Figure 6 to compare the relationship between valve closing time and water hammer pressure at different flow velocities.

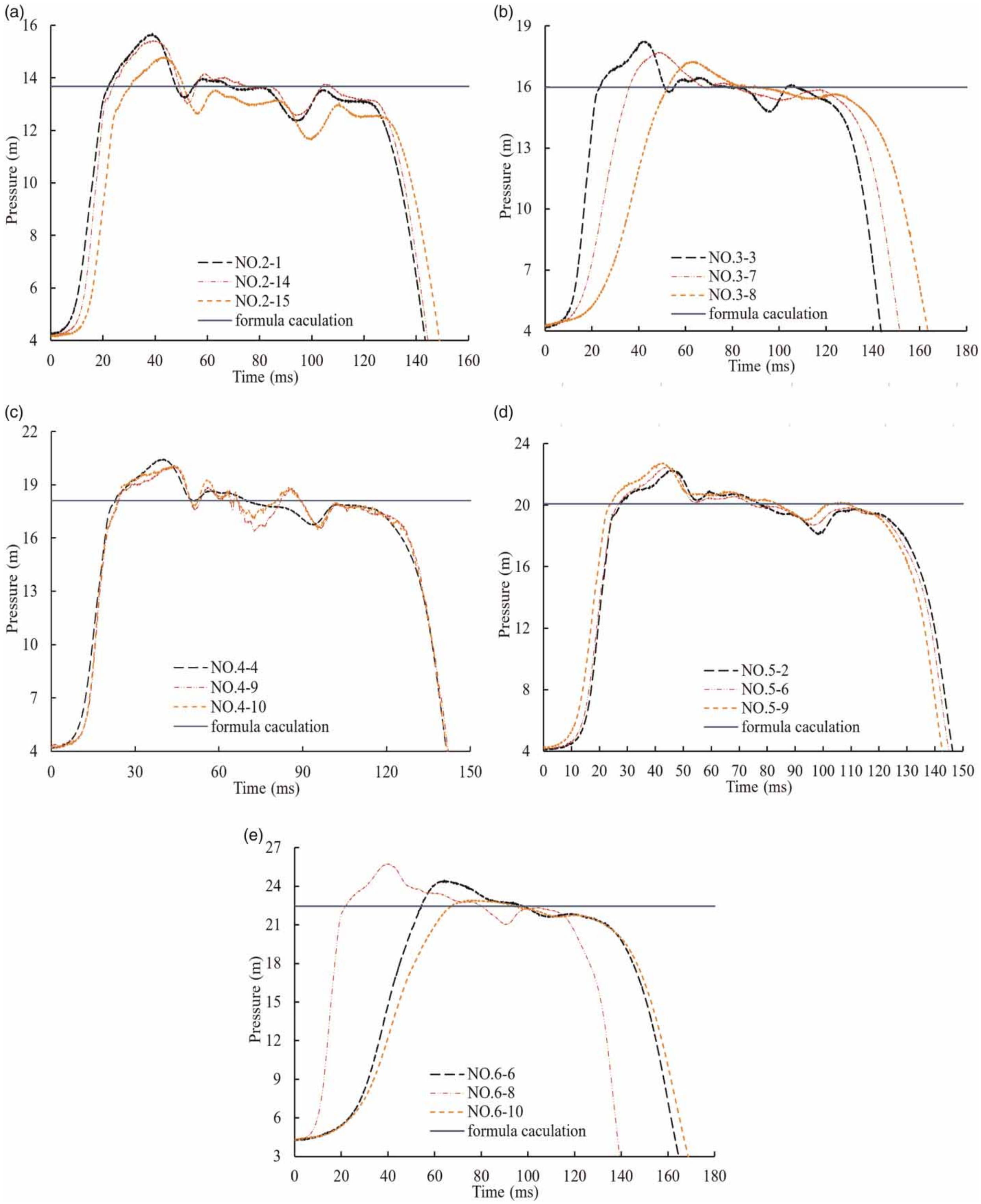

Figure 6 | First positive wave of water hammer at different flow velocities: (a) $V = 0.147$ m/s; (b) $V = 0.183$ m/s; (c) $V = 0.216$ m/s; (d) $V = 0.247$ m/s and (e) $V = 0.284$ m/s.

The results show when $V = 0.147$ m/s (Figure 6(a)), the closing time of the valve is from 37 to 40 to 46 ms, the extreme value of water hammer pressure was from 15.69 to 15.43 to 14.78 m, the closing time of the valve was increased by 9 ms and the water hammer pressure was reduced by 0.91 m. When $V = 0.183$ m/s, Figure 6(b) shows that when the closing time of the valve was from 42 to 51 to 65 ms, the maximum pressure was from 18.23 to 17.71 m, the closing time of the valve increased by 23 ms and the pressure decreased by nearly 1 m, indicating that the influence of the closing time of the valve on the water hammer pressure cannot be neglected. When $V = 0.216$ m/s (Figure 6(c)), the closing times of the valve of the three groups were 40, 46 and 44 ms respectively, and the maximum pressure were 20.44, 20.01 and 20.10 m respectively. Since the closing time of the valve of the three groups was close to each other with difference in 6 ms, the maximum pressure after valve closing was not much different than 0.43 m. However, a shorter the closing time of the valve caused a greater water hammer pressure. When $V = 0.247$ m/s (Figure 6(d)), as the closing time of the valve decreased from 48 to 43 ms, the maximum pressure increased from 22.26 to 22.73 m, the closing time of the valve was shortened by 5 ms and the water hammer pressure increased by 0.47 m. When $V = 0.283$ m/s (Figure 6(e)), the maximum pressure decreased from 25.73 to 22.91 m with the increase of valve closing time from 41 to 78 ms, and the maximum pressure decreased by 2.82 m with the increase of closing time of the valve by 37 ms. According to the above test results, the water hammer of the viscoelastic pipeline was related to the closing time of valve. The water hammer increased with decrease of the closing time of valve.

To quantitatively analyze the influence of closing time of the valve on water hammer, three flow velocities were selected to compare the traditional pressure rise of water hammer with the measured pressure rise under different conditions. The relationship between percentage of direct water hammer pressure rise and relative closing time of the valve is shown in Figure 7.

As shown in Figure 7, the percentage of direct water hammer pressure rise varies in the same trend with the relative closing time of the valve under different flow rates. A smaller closing time of the valve caused a larger percentage of water hammer pressure over the theoretical value. When $V = 0.11$ m/s, T_t/T_c varies from 0.5 to 0.32 (the closing time of the valve decreases from 60 to 38 ms) and the percentage beyond the traditional value $(H_t - H_c)/H_c$ increases from 5.71 to 20.06%. When $V = 0.183$ m/s, T_t/T_c varies from 0.67 to 0.35 (the closing time of the valve decreases from 80 to 42 ms) and $(H_t - H_c)/H_c$ increases from 1.94 to 18.84%. When $V = 0.284$ m/s, T_t/T_c varies from 0.65 to 0.35 (the closing time of the valve decreased from 78 to 42 ms) and $(H_t - H_c)/H_c$ increases from 2.49 to 17.20%. The results indicated that the closing time of the valve has a great influence on the pressure rise in the viscoelastic pipeline. Water hammer pressure increased with decrease of the closing time of valve. The percentage beyond the traditional pressure rise increased with increase of the difference between the measured pressure rise and the traditional calculated value of the water hammer. Due to closing the valve rapidly, the pipe

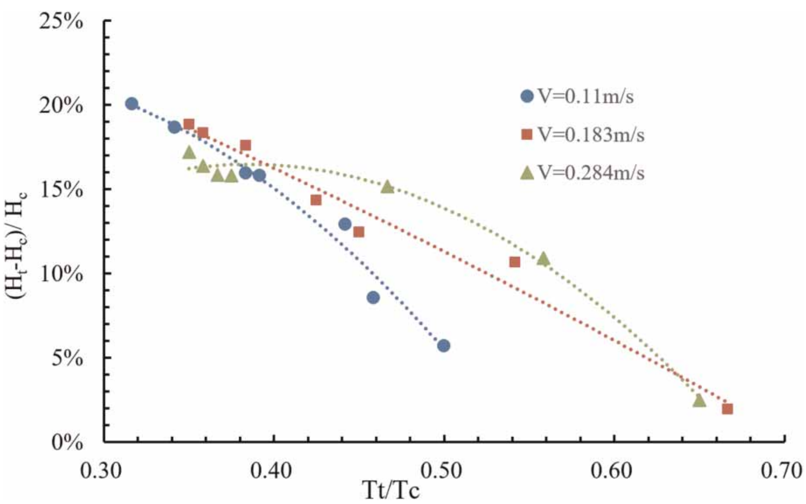

Figure 7 | Relationship between percentage of direct water hammer pressure rise and relative value of valve closing time. *Note:* T_t is the closing time of valve measured in tests; T_c is the longest time for direct water hammer, 120 ms; H_t is the water hammer measured in tests; H_c is the traditional water hammer in Formula (1).

could not react instantly. When the stress was constant and the strain was small, the 'rigidity' of the pipe was large. With increase of the modulus of elasticity, the wave velocity value was larger, so as to measure a larger water hammer pressure.

CONCLUSIONS

In this paper, the direct water hammer characteristics in the viscoelastic pipeline were studied by physical tests. The following conclusions were drawn:

1. In the viscoelastic pipes, such as the PMMA, water hammer was different from the traditional direct water hammer theory. The measured water hammer pressure was 15–20% greater than the traditional value.
2. The water hammer of the viscoelastic pipeline was related to the closing time of valve. A shorter closing time of the valve caused a greater water hammer pressure. Then the difference was larger compared with the traditional calculation value.
3. Due to the elastic aftereffect of viscoelastic pipe, stress and strain were out of sync when the valve was closed quickly. The lag of strain made the elastic modulus of the pipe large at the time of valve closing, which led to a large wave velocity. Then a greater water hammer eventually was generated. When the valve was closed faster, the less time the pipe had to produce strain, which resulted in a higher elastic modulus and the greater water hammer pressure.
4. The physical apparatus is a preliminary test with a single long straight pipe. In the future, we will further study water hammer experiment with different kinds of viscoelastic pipes in different layouts with different diameters of the pipes.

ACKNOWLEDGEMENTS

This work was sponsored by the Natural Science Foundation of Xinjiang Uygur Autonomous Region (Grant No. 2021D01B57), the Xinjiang Key Laboratory of Hydraulic Engineering Security and Water Disasters Prevention Open Project in 2021 (Grant No. ZDSYS-JS-2021-08) and the National Natural Science Foundation of China (Grant No. 51879087).

DATA AVAILABILITY STATEMENT

All relevant data are included in the paper or its Supplementary Information.

REFERENCES

Bergant, A., Tijsseling, A. S., Vítkovský, J. P., Covas, D. I. C., Simpson, A. R. & Lambert, M. F. 2008 Parameters affecting water-hammer wave attenuation, shape and timing – part 1: mathematical tools. *Journal of Hydraulic Research* **46** (3), 373–381.

Brunone, B. & Golia, U. M. 2008 Discussion of 'Systematic evaluation of one-dimensional unsteady friction models in simple pipelines' by Vítkovský, J. P. Bergant, A., Simpson, A. R., & Lambert, M. F. *Journal of Hydraulic Engineering* **134** (2), 282–284.

Chaudhry, M. H. 1979 *Applied Hydraulic Transients*. Van Nostrand Reinhold Co. Springer, New York, NY.

Chen, X., Zhang, J., Yu, X., Chen, S. & Shi, L. 2021 Study on impedance size optimization of a one-way surge tank in a long-distance water supply system. *Water Supply* **21** (2), 868–877.

Covas, D., Stoianov, I., Ramos, H., Graham, N. & Maksimovic, C. 2004 The dynamic effect of pipe-wall viscoelasticity in hydraulic transients. Part I experimental analysis and creep characterization. *Journal of Hydraulic Research* **42** (5), 517–532.

Duan, H., Ghidaoui, M. S. & Tung, Y.-K. 2010 Energy analysis of viscoelasticity effect in pipe fluid transients. *Journal of Applied Mechanics* **77** (4), 044503.

Duan, H., Che, T., Lee, P. J. & Ghidaoui, M. S. 2018 Influence of nonlinear turbulent friction on the system frequency response in transient pipe flow modelling and analysis. *Journal of Hydraulic Research* **56** (4), 451–463.

Duan, H., Pan, B., Wang, M., Chen, L., Zheng, F. & Zhang, Y. 2020 State-of-the-art review on the transient flow modeling and utilization for urban water supply system (UWSS) management. *Journal of Water Supply: Research and Technology – AQUA* **69** (8), 858–893.

Franke, P.-G. 1983 Computation of unsteady pipe flow with respect to visco-elastic material properties. *Journal of Hydraulic Research* **21** (5), 345–353.

Gally, M., Güney, M. & Rieutord, E. 1979 An investigation of pressure transients in viscoelastic pipes. *Journal of Fluids Engineering* **101** (4), 495–499.

Gong, J., Zecchin, A. C., Lambert, M. F. & Simpson, A. R. 2016 Determination of the creep function of viscoelastic pipelines using system resonant frequencies with hydraulic transient analysis. *Journal of Hydraulic Engineering* **142**, 04016023.

Gong, J. Z., Stephens, M. L., Lambert, M. F., Zecchin, A. C. & Simpson, A. R. 2018 Pressure surge suppression using a metallic-plastic-metallic pipe configuration. *Journal of Hydraulic Engineering* **144** (6), 04018025.

Miao, D., Zhang, J., Chen, S. & Yu, X. 2017 Water hammer suppression for long distance water supply systems by combining the air vessel and valve. *Journal of Water Supply: Research and Technology – Aqua* **66** (5), 319–326.

Pan, B., Duan, H., Meniconi, S., Urbanowicz, K., Che, T. C. & Brunone, B. 2020 Multistage frequency-domain transient-based method for the analysis of viscoelastic parameters of plastic pipes. *Journal of Hydraulic Engineering* **146** (3), 04019068.

Pezzinga, G., Brunone, B. & Meniconi, S. 2016 Relevance of pipe period on Kelvin-Voigt viscoelastic parameters: 1D and 2D inverse transient analysis. *Journal of Hydraulic Engineering* **142** (12), 04016063.

Thorley, A. R. D. 2004 *Fluid Transients in Pipeline Systems*. ASME Press, London.

Tran, P. D. 2017 Pressure transients caused by air-valve closure while filling pipelines. *Journal of Hydraulic Engineering* **143** (2), 04016082.

Trikha, A. K. 1975 An efficient method for simulating frequency dependent friction in transient liquid flow. *Journal of Fluids Engineering* **97** (1), 97–105.

Triki, A. 2018 Further investigation on water-hammer control inline strategy in water-supply systems. *Journal of Water Supply: Research and Technology – AQUA* **67** (1), 30–43.

Urbanowicz, K., Duan, H. F. & Bergant, A. 2019 Transient flow of liquid in plastic pipes. *Journal of Mechanical Engineering* **66** (2), 77–90.

Vardy, A. E. & Brown, J. M. B. 1995 Transient, turbulent, smooth pipe friction. *Journal of Hydraulic Research* **33** (4), 435–456.

Wineman, A. S. & Rajagopal, K. R. 2000 *Mechanical Response of Polymers: An Introduction*. Cambridge University Press, New York, USA.

Wylie, E. B., Streeter, V. L. & Suo, L. 1993 *Fluid Transients in Systems*. Prentice Hall, Englewood Cliffs, NJ, USA.

First received 6 January 2022; accepted in revised form 20 March 2022. Available online 1 April 2022